Peer-reviewed version available at *Recycling* **2018**, *3*, 57; doi:10.3390/recycling3040057

Characterization of Feedstock Filament Extruded from Secondary Sources of PS, ABS and PVC

Turku Irina[1]✉, Kasala Sushil[1] and Kärki Timo[1]

[1]Fiber Composite Laboratory, School of Energy Systems, Lappeenranta University of Technology, Lappeenranta, Finland

✉Corresponding author: Irina.Turku@lut.fi

Abstract

The recyclability of polystyrene, acrylonitrile butadiene styrene, polystyrene and polyvinylchloride waste and using them as a source for 3D printing were studied. Filaments of about 3 mm in diameter were extruded successfully with a small-size extruder. The processed filaments were tested on a broad range of parameters - glass transition temperature, tensile properties and a pyrolysis scenario were obtained. The measured parameters were compared with parameters of virgin counterparts presented in the literature. In order to estimate the toxicity of the recycled material, elemental analysis of the samples was done.

Keywords: plastic recycling, filament extrusion, tensile property, thermal analysis

1. Introduction

Plastic, being a highly versatile and resource-efficient material, has become unreplaceable material in many economic sectors, such as packaging, building and construction, transportation, and renewable energy, among others [1]. The growing plastic production and consumption have led to an increasing dependence of plastic production from fossil fuel, the main resource for plastic manufacturing, as well as in an increase of plastic waste. Statistics show that of the 27.1 million tons of post-consumer plastic collected in 2016, 31.1% was recycled, 41.6 % incinerated and 27.3% landfilled. Thus, a large portion of plastic is still landfilled; however, this was the first time in Europe when recycling overcame landfill [1]. In the EU commission Action Plan for a circular economy from 2015, plastic production is identified as a key priority [2]. The circular plastic economy vision is based on the need of innovative solutions for developing new sustainable products, durable with a long lifespan, and being high quality recyclable products after use. Among other waste management options, mechanical recycling of plastics is the most resource-effective, providing also more

jobs than landfilling or incineration [3]. However, mechanical recycling can be limited by the presence of toxic components in the recyclant [4,5].

Recently, 3D printing technology, related to additive or direct manufacturing, has developed rapidly, raising interests in many fields of business and household services. Unlike conventional manufacturing, direct manufacturing makes it possible to move from product design with computer-aided design (CAD) models to fabrication without intermediate stages. Such flexibility in design options allows to organize manufacturing at small companies, e.g. home 3D printing and *local fabrication* at a printshop [6]. Yet, 3D printing is a way for effective use of raw materials, minimizing waste and saving energy and other resources. Moreover, using "household"-scale recycling systems can be an alternative to centralized recycling due to the fact that some negative environmental impacts can be overcome. The collection, transport and transfer (CTT) of recyclable waste plays a significant part in greenhouse gas emissions from the total global warming potential of the recycling process [7].

The rapid development of 3D printing technology includes also development of the technology of 3D printer filaments. Today, multiple companies are specialized in the production and distribution of them [8,9]. The most popular plastics in 3D printing technology are polylactic acid (PLA) and acrylonitrile-butadiene-styrene (ABS). Local recycling presumes that the filaments are produced from local recycled material and the quality of this material influences its recyclability, e.g. the quality of the final product. Examples of virgin and secondary plastic waste processing by using a small-scale filament extruder that converts plastic (chips, particles) into filament can be found in the literature [7,10,11].

The main aim of this study was to estimate the recyclability of acrylonitrile butadiene styrene (ABS), polystyrene (PS) and polyvinylchloride (PVC) plastic waste, i.e. to measure the mechanical and physical properties of filaments manufactured from these plastics and to compare them with virgin grades. In addition, possible chemical contaminants that can be present in plastic waste were also estimated. Plastic waste was collected from a local landfill or obtained from commercial companies. The plastics were separated into singular plastic grades. The samples for testing were manufactured by using a Filabot extruder. The extruded material was studied for its mechanical properties (tensile strength and modulus), melt flow index, and glass transition temperature, and a thermal degradation scenario was obtained. Elemental analysis of the samples was performed by using energy-

dispersive X-ray spectroscopy (EDS). Emitted volatiles during pyrolysis were measured by a mass spectrophotometer (MS).

2. Materials and methods

2.1 Plastic sources and filament manufacturing

The materials were obtained from the company Etelä-Karjalan Jätehuolto Oy (Lappeenranta, Finland) and Destaclean Oy. From the mixed plastic waste, three plastic types, ABS, PVC and PS were extracted by using a Near Infrared (NIR) spectroscopy device (Thermo Scientific™ MicroPHAZIR™ PC Analyzer for Plastic). The plastic fragments were reduced to 2 cm - sized flakes and then extruded by using a low speed extruder Filabot EX2 (Shini). The PVC filaments were extruded at 196 °C, PS at 200 °C and ABS at 180 °C constant temperatures. The extrusion flow rate was adjusted manually for each material. The diameter of the extruded filament was approx. 3 mm.

2.2 Melt flow index

Experimental melt flow index (MFI) was measured by using Dynisco LMI 5000 (Dynisco) in accordance with standard EN ISO 1133-1. The MFI of ABS and PS was measured at 220 °C and 200 °C, respectively.

2.3 Fourier-transform infrared analysis

Extruded filaments were analyzed with the Fourier-transform infrared (FTIR) technique. An FTIR spectrometer (Perkin-Elmer, UK) equipped with an attenuated total reflection (ATR) device (MIRacle PIKE Technologies) with zinc selenide crystal was used. The spectra were collected by co-adding 4 scans at a resolution of 4 cm^{-1} in the range from 4000 to 400 cm^{-1}.

2.4 Tensile property testing

The tensile tests of the filaments was performed according to EN-310 standard (adapted to a filament-shape sample) on a Zwick Z020 machine. The cross-head speed was 2 mm/min for modulus testing and 50 mm/min for the other measurements. The gauge length was 25 mm. The test samples, 120 mm long filaments were cut from a trial sample, conditioned according to above standard. Tests were carried out with 12 sample replicates.

2.5 Differential scanning calorimeter and thermogravimetric analysis

Thermal analysis measurements were performed by mean a differential scanning calorimeter (DSC), and thermogravimetric analysis (TGA) with a linear temperature increase (Netzsch DSC TGA 204 F1 Phoenix®). DSC was performed under a nitrogen atmosphere, at a 40 mL/min flow rate and heating rate 10 °C/min. The sample, approx. 10 mg, was placed in an aluminum pan and heated from 25 to 200 °C and then cooled down to 25 °C after keeping at 200 °C for 10 min. This procedure was done twice, and the thermogram of the second scan was used for the analysis. For thermogravimetric analysis, approx. 10 mg of the specimen was heated from 25 °C to 800 or 900 °C at a rate of 10 °C/min under helium atmosphere of 40 mL/min at constant flow rate. Evolved gas emission (EGA) during TGA was analyzed by using a mass spectrophotometer (MS) which was coupled with TGA. The MS analysis was limited to 160 m/z. The results were interpreted with Proteus and Aeolos software. For further EGA spectra interpretation, the database "NIST Chemistry WebBook 69" was used [12].

3. Results and discussion

3.1 Melt flow index

The rheological behavior of the polymer is important in material processing. MFI, i.e. the mobility of polymer chains, commonly defines the operational temperature for extrusion, injection molding and blow molding. Concerning 3D printing, MFI and the operational temperature are also important parameters due to their influence on the degree of layer adhesion.

Table 1 presents the measured MFI parameters for the recycled polymers and parameters found in the literature for virgin ones. According to the results, the MFI value of recycled ABS was significantly lower than that of the virgin one, 8.9 and 30 g/10 min, respectively. The MFI of the PS, 11.5 g/10 min, was very close to the virgin grade, 12-16 g/10 min. The MFI of virgin rigid PVC (190 °C/21.6 kg) varies from 1.4 to 60 g/10 min [16]. The attempts to measure the MFI of recycled PVC were not successful due to the material degrading and clogging the equipment during testing. MFI is sensitive to environmental impact and thermomechanical stress, e.g. during lifespan and reprocessing. Jin et al. who studied the influence of multiple extrusion on the flow properties of low-density polyethylene (LDPE) reported that MFI decreased from 2.31 g/10 min to 0.02 g/10 min after 100

extrusions [17]. This change was attributed to chain scission or crosslinking of the polymer chains.

3.2 Fourier-transform infrared analysis

Infrared spectra of the rABS, rPS and rPVC samples are shown in Figure 1. Comparative analysis of the samples with virgin counterparts, spectra available in the literature, show that the samples are homogeneous, e.g. without noticeable impurities. The similarity in the molecular structure of ABS and PS, Figure 2, is also reflected in the similarity of their FTIR spectra. The characteristic peaks of ABS and PS, the C-H stretching vibration aromatic, at 3200-3000 cm^{-1}, and aliphatic, at 3000-2800 cm^{-1}, are clearly observed in both spectra. The band at 2237 cm^{-1} corresponds to the C≡N bond observed in the ABS spectra. The band at 1736 cm^{-1}, oxygen containing carbonyl groups (C=O) band is probably due to an oxidation process in the polymers during usage [18]. The peaks at 1602 cm^{-1} and 1592 cm^{-1} correspond to C=C aromatic double bond stretching vibration. The absorptions at 1493 cm^{-1} and 1452 cm^{-1} are also due to carbon–carbon stretching vibrations in the aromatic ring. However, the band at 1452 cm^{-1} may have resulted from both ring breathing of the benzene ring and the deformation vibration of $–CH_2$ [19]. The peaks at 1070 cm^{-1} and 1028 cm^{-1} are in-plane C-H bending of the aromatic ring. The two peaks at 757 cm^{-1} and 697 cm^{-1} are due out-of-plane aryl C-H bending for the (mono)substituted benzene ring. The absorbance bands at 966 cm^{-1} and 911 cm^{-1} in the ABS spectra correspond to C=C unsaturation (vinyl) in polybutadiene, and the 1,2 butadiene terminal vinyl C-H band, respectively [20]. The PVC spectra are characterized by aliphatic C-H stretching vibration, 3000-2800 cm^{-1}, the peak at 1452 cm^{-1} is due to $-CH_2$ stretching vibration, and the peaks near 612 cm^{-1} and 691 cm^{-1} are due to C-Cl stretching vibration [21]. This spectrum also reveals the absence of phthalates, which have a specific region at 1620-1560 cm^{-1} [22]. Thus, this is consistent with the TGA-MS analysis, which also did not reveal phthalate emitting (see the section below). The peaks at 1430 cm^{-1} and 880 cm^{-1} might belong to calcium carbonate $CaCO_3$ [23], the presence of which, i.e. Ca-ion, was detected by EDS analysis (see Table 2). Ca-ion was also detected in the other samples, but in much smaller amounts than in PVC, which was the reason for the absence of $CaCO_3$ specific regions in the IR spectra of ABS and PS. The ageing sign of rPVC could be detected by the presence of a peak near 1740 cm^{-1}, the carbonyl groups region.

3.3 Differential scanning calorimeter and thermogravimetric analysis

Peer-reviewed version available at Recycling 2018, 3, 57; doi:10.3390/recycling3040057

The glass transition temperature, T_g, and specific heat in the glass transition, ΔC_p, of the tested polymers and their virgin counterparts found in the literature, are listed in Table 3. As can be seen, the T_g of recycled polymers is lower than that of virgin ones. The main reason for T_g changing is usually thermomechanical impact during reprocessing, as well as different external factors during material usage. During ageing, as known, random thermal scission or crosslinking can occur, which in turn decreases or increases T_g, respectively. However, changes in the T_g for recycled materials cannot be attributed solely to ageing due to other factors, as e.g. contaminants or additives, which are often present in recycled materials, can have an influence on the T_g parameter.

3.4 Heat resistance and thermal stability

Experimental results of the thermal degradation of the polymers, mass losses and the corresponding DTG curves, are shown in Figure 3. As can be seen, PVC has a significantly faster mass loss rate compared to the ABS and PS grades. The sensitivity of PVC to heat is mostly related to the low binding energy of the C-Cl and thus process dechlorination starts at lower temperatures [25]. The low thermal stability of PVC is also associated with defects presence in the PVC structure, e.g. allylic and tertiary chloride moieties, which are formed during PVC polymerization [26]. This instability of PVC toward heat is compensated by leaving a large char portion at the end of pyrolysis. Char formation can be attributed to forming of reactive carbonium-ion centers in the polymer, which act as an active center for crosslinking and char building [27].

Unlike in the other samples, the mass loss curve of PVC shows two steps, at the temperature region from 210 °C to 360 °C and from 360 °C to 540 °C, with peaks at 282 °C and 454 °C for the first and second steps, respectively (Figure 3). The mass losses were about 58 wt% in the first step and in the second step about 83 wt% as a whole. Large amount of residue was formed due to carbonaceous char formation and presence of inorganic additives [28]. In general virgin PVC burns incompletely under inert atmosphere, leaving about 10 wt% of carbon-rich char [28,29,30]. Basis on this, the inorganic part of PVC can be estimated as about 7 wt%. Two-step mass loss during PVC pyrolysis is well known and has been described in various reports [31,32]. Briefly, the decomposition of PVC starts from dehydrochlorination, elimination of HCl, followed by benzene formation through cyclization of $(CH=CH)_n$ [33]. This process is displayed schematically in Figure 4. Along with HCl and benzene, many other volatiles are generated during PVC burning, and can be detected with

FTIR, gas chromatography (GC) and MS analyzers or their combinations [31,32,34,35]. In this study, the probable gas emission was estimated on the basis of the masses to charge ratios (*m*/*z*) of the volatiles released, and interpreted by using the "NIST Chemistry WebBook 69" data base [12] and compared with published results found in the literature. According to the emitted gas analysis, two main components, Cl (*m*/*z* 35), (*m*/*z* 36, 38) and benzene (*m*/*z* 77, 78), were emitted during the first degradation step, see Figure 5. Intensive water vapor, a peak at *m*/*z* 17, 18, and a large peak at *m*/*z* 44 due to CO_2 evolution were also detected. Oxygen-containing gases can probably be formed due to the presence of O-containing additives. The presence of O-ion in the PVC was detected by EDS analysis (see the chapter below). Xu et al. defined CO_2 generation in the presence of ferrites, O-containing fire retardants, whereas pure PVC did not emit CO_2 during pyrolysis in the inert atmosphere [29]. A few peaks at m/z 39-65 can be attributed to the generation of light aliphatic hydrocarbons, C_2-C_5 (*m*/*z* 39-65), also including chlorinated ones [28]. McNeill et al. studied virgin PVC thermal degradation and found evolution of aliphatic hydrocarbons, namely C_{10}-C_{13} alkenes (*m*/*z* 55-57) and cyclopentene (*m*/*z* 67) [30]. The second step of PVC degradation, which is clearly distinguishable in the mass loss curve and the related gas emission diagram is due to increased emission of aliphatic hydrocarbons as well as cyclic compound generation. Along with benzene (*m*/*z* 77, 78), other aromatic compounds, toluene (*m*/*z* 91, 92), styrene (*m*/*z* 51, 78, 104), C_3-C_5 alkyl benzenes (*m*/*z* 105) and ethylbenzene (*m*/*z* 104), and the isomers of xylene (m/z 106) were formed [30]. It can be said that these aromatic components were formed during the first step in small amounts, with significantly increased amounts during the second step, observed previously for virgin PVC pyrolysis [30]. Phthalates, which are often used in PVC manufacturing as plasticizers, were not detected. Phthalates can be identified by the presence of a peak at *m*/*z* 149 [33]. This is in line with the FTIR analysis, which did not detect a peak associated with phthalates either. In this study, rigid PVC from water tube PVC waste was used, where the amount of plasticizers should be very insignificant.

PS is a homopolymer where styrene is the monomer, see Figure 2. PS had one-step mass loss scenario with onset at 360 °C and offset at 500 °C, showing a DTG peak at 426 °C. The PS sample decomposed almost completely, with 2 wt% residual material left. In general, pure PS burns completely without char, which was reported in various studies [34,35,36]. The small residue in our case can be attributed to the additives and possible contaminants that can be present in recycled materials. Mass spectrometry analysis of the evolved gases (Figure 5) showed ion currency peaks at 39, 51, 63, 65, 78, 91, 104, 117, 118

and 130 *m*/*z*. The signals at 51, 78 and 104 *m*/*z* belong to the styrene monomer; the peaks at 77 and 78 *m*/*z* originated from benzene; the peaks at 91 and 92 *m*/*z* came from toluene; and the signals at 118 and 130 *m*/*z* might belong to methylstyrene and phenylbutadiene, respectively [37]. Seleem et al. report that PS was pyrolyzed to toluene, styrene, benzaldehyde, and 4-phenyl-1-butyne [36].

The ABS polymer is a complex molecule composed of acrylonitrile (15 wt%), butadiene (40 wt%) and styrene (45 wt%). The ABS molecule monomer is shown schematically in Figure 2. The sample showed one-step mass loss which started from 360 °C and completed at about 500 °C, leaving a residue of about 4 wt%. The peak of mass loss was at 420 °C. This is consistent with a previously published result [37]. The evolved gas analysis of rABS showed that possible gases were acrylonitrile (*m/z* 53), benzene (*m/z* 77, 78), styrene (*m/z* 51, 78, 104), toluene (*m*/*z* 91, 92) and methylstyrene (*m*/*z* 118). The one-step pyrolysis of ABS was consistent with other published results [31,38]. However, in the quasi-isothermal TGA method, where the TGA instrument was programmed to heat the sample at the following isothermal step, multicomponent ABS showed more than one step mass loss due to the possibility of separation of overlapped decomposition events [38]. It was shown that ABS decomposed first styrene acrylonitrile, followed with butadiene (m/s 54). In another study, the researchers showed that ABS generated first butadiene, starting from 340 °C, then styrene at 350 °C, and acrylonitrile starting at about 400 °C [31]. According to Vouvoudi et al., ABS starts to degrade from the abstraction of the side –CN groups [39]. Vouvoudi et al. studied the pyrolysis of recycled ABS from waste electrical and electronic equipment (WEEE), and showed that ABS had a three-step mass loss curve where acetonitrile, acrylonitrile and styrene emission, along with several aromatic compounds with 1, 2 or 3 phenyl rings and substituted nitriles were detected [39].

3.5 Scanning electron microscope - energy dispersive X-ray spectroscopy analysis

Energy dispersive X-ray spectroscopy (EDS) is a fast method for the analysis of constituent elements. The elemental composition detected in the polymers is shown in Table 2. In PVC, as expected, the share of chlorine (Cl) is high, about half of the total sample weight. Elements such as Mg, Ca, Ti, Al and oxygen originated from additives that are usually applied in plastic production. Metal-containing fire-retardant $Mg(OH)_2$ and $Al(OH)_3$, Ca-based stabilizers and pigment (TiO_2) were also detected. In fact, a large amount of Ca

belongs to a Ca-based stabilizer which is widely applied in PVC manufacturing [43]. The small amount of silicon, Si, which is a component of sand, can have originated from soil impurities. In addition, small amounts of Na, K, Fe and Cu were detected in ABS.

3.6 Mechanical properties

The extruded filaments were tested for their tensile properties. Experimental results and values for the virgin counterparts taken from the literature are listed in Table 4. As can be seen, the tensile strengths of recycled PS and ABS were much smaller than those of the virgin ones. The tensile strength of rPVC, however, was comparable with the tensile strength of plasticized virgin PVC. Elongation at break, in turn, was significantly smaller. It could be noted that the shape of the sample, i.e. filament, differs from the dimensions listed in the related standard. For filaments, mostly tear strength values are shown in polymer filament in specifications.

Conclusions

Filament samples, about 3 mm in diameter, were extruded with a small-scale extruder from recycled polystyrene (PS), acrylonitrile butadiene styrene (ABS) and polyvinylchloride (PVC) materials. Fourier-transform infrared spectral analysis of the material confirmed the purity of the studied samples. Thermal analysis showed that the glass transition temperatures of the recycled PS, ABS and PVC were very close to their virgin counterparts. The melt flow index (MFI) of rPS was similar to virgin PS, whereas the MFI of rABS was significantly lower than that of virgin ABS; MFI of PVC was not detected. The pyrolysis of the samples revealed that PVC burned incompletely, leaving about 17 wt% of char (carbon-reach and inorganic components), whereas PS leaved about 2 wt%, and ABS about 4 wt% of solid residue. On the basis of this it can be concluded that PS and ABS contained about 2 and 4 wt% of inorganic additives/contaminants, respectively. The inorganic part of PVC can be estimated as about 7 wt% due to fact that virgin PVC burn incompletely under inert atmosphere, leaving about 10 wt% of carbon-rich char. The mechanical testing showed that the tensile properties of rPS and rABS were significantly lower than those of the virgin counterparts, whereas rPVC was mechanically comparable with pure PVC. The analysis of gases evolved during pyrolysis showed that the studied plastics decomposed in accordance with a scenario similar to their virgin counterparts.

Preprints (www.preprints.org) | NOT PEER-REVIEWED | Posted: 24 October 2018 doi:10.20944/preprints201810.0581.v1

Peer-reviewed version available at Recycling 2018, 3, 57; doi:10.3390/recycling3040057

Based on the results it can be concluded that studied recycled material can substitute virgin material is some undemanding applications. However, the next stage, i.e. samples 3D printing with following mechanical testing have to be performed.

Table 1. Parameters of extruded filaments for recycled samples and their virgin counterparts found in the literature.

Material/Parameter	T_{extr} (°C)	*d* (cm)	MFI (g/10 min)	MFI, virgin (g/10min)
ABS	180	3.81(0.12)	8.9(0.8)	28 [13], 30 [14]
PS	200	2.98(0.08)	11.5(0.9)	12-16 [15]
PVC	196	3.57(0.14)	N/A	1.4-60 [16]

Table 2. Elemental composition of rABS, rPS and rPVC, wt%; standard deviation is given in parentheses.

Material/ element	C	O	Cl	Mg	Al	Ca	Na	Ti	Si	S	K	Fe,Cu
ABS	86(8)	3(2)	0.3(0.1)	0.02(0.03)	1.1(0.4)	0.2(0.1)	0.2(0.1)	0.7(0.3)	0.1(0.06)	0.04(0.04)	0.3(0.1)	<0.02
PS	98(0.4)		0.14(0.02)		0.7(0.4)	0.1(0.03)	0.1(0.1)	0.6(0.1)	<0.1			
PVC	57(6)	4(0.6)	37(9)	<0.01	0.6(0.1)	1.3(0.1)			0.1(0.01)	0.02(0.01)		

Table 3. Thermal parameters of rABS, rPS and rPVC.

Material/ property	T_g (°C)		T_g virgin (°C) [24]
	II cyc	III cyc	
rABS	106.4	106.5	80-125
rPS	87.5	85.6	100
rPVC	81	80.9	87

Table 4. Tensile properties of extruded filaments from recycled materials and virgin counterparts taken from internet database [41].

Material/ property	Tensile, measured			Tensile, virgin	
	Strength, MPa	Modulus, GPa	Elongation at break, %	Strength, MPa	Elongation at break,%
rABS	14.5(1)	2.7(2.8)	2(2)	34	6
rPS	4.3(0.35)	1.85(0.4)	1(1)	34	1.6
rPVC	17(1)	2.9(0.1)	8(8)	14-20*	95-280*

*plasticized PVC

Preprints (www.preprints.org) | NOT PEER-REVIEWED | Posted: 24 October 2018 doi:10.20944/preprints201810.0581.v1

Peer-reviewed version available at Recycling 2018, 3, 57; doi:10.3390/recycling3040057

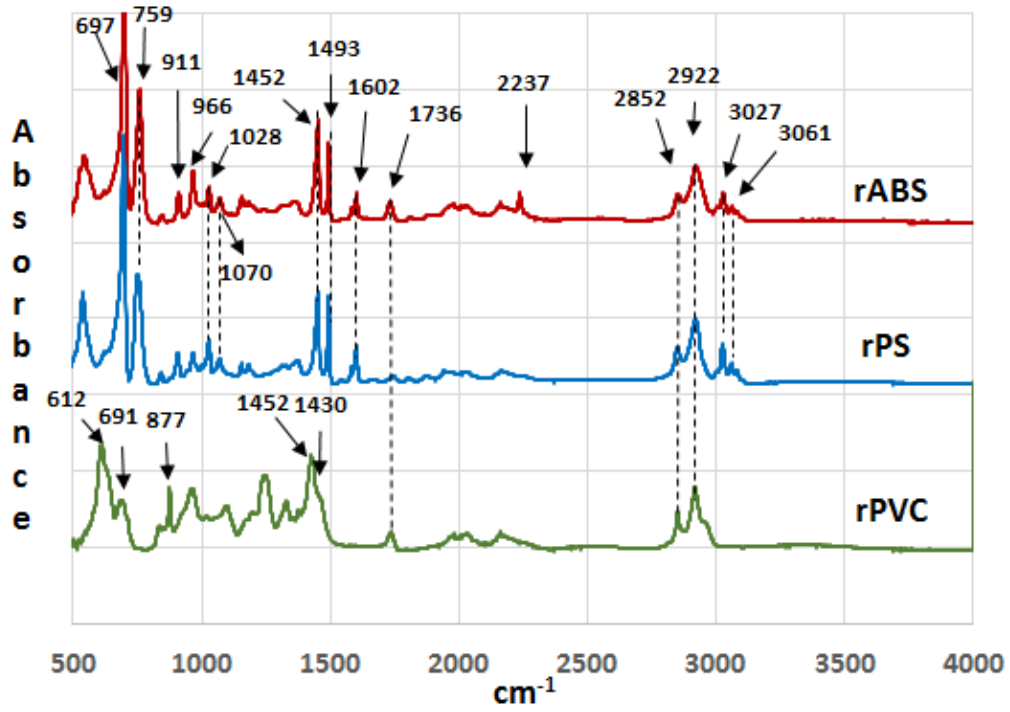

Figure 1. Infrared spectra of rABS, rPS and rPVC.

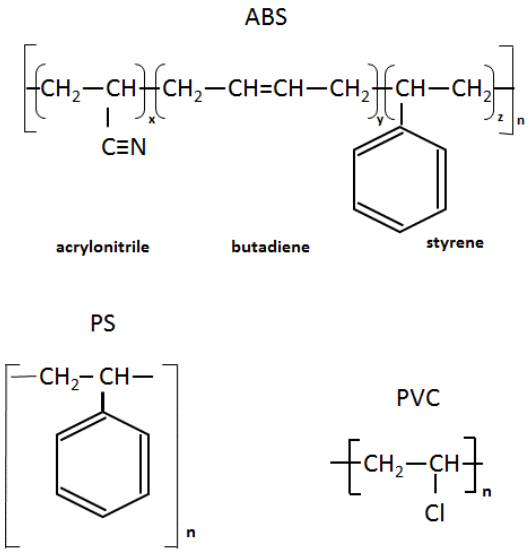

Figure 2. Chemical structure of ABS, PS and PVC.

Preprints (www.preprints.org) | NOT PEER-REVIEWED | Posted: 24 October 2018 doi:10.20944/preprints201810.0581.v1

Peer-reviewed version available at Recycling 2018, 3, 57; doi:10.3390/recycling3040057

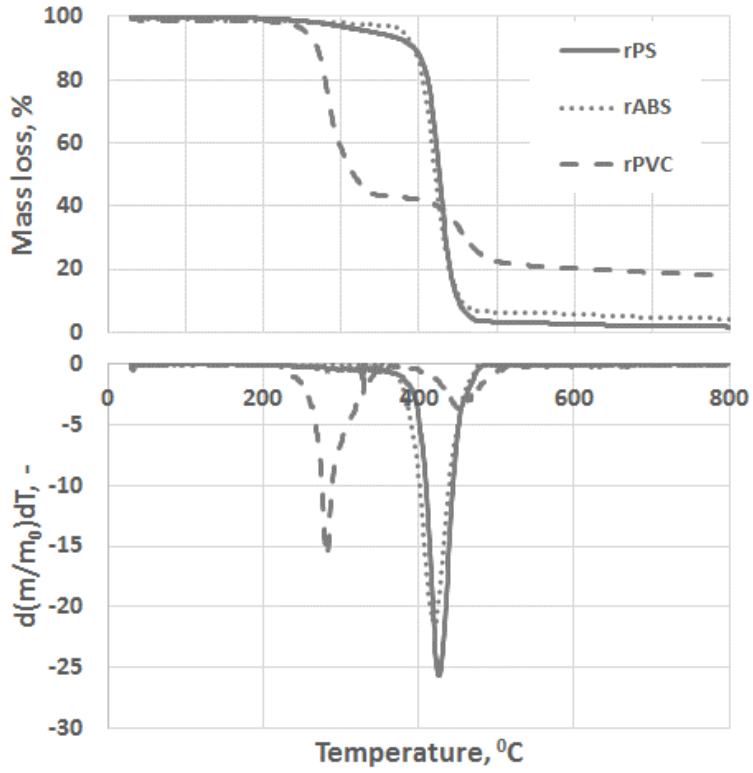

Figure 3. TGA and DTG curves of rPS, rABS and rPVC pyrolysis under a neutral atmosphere.

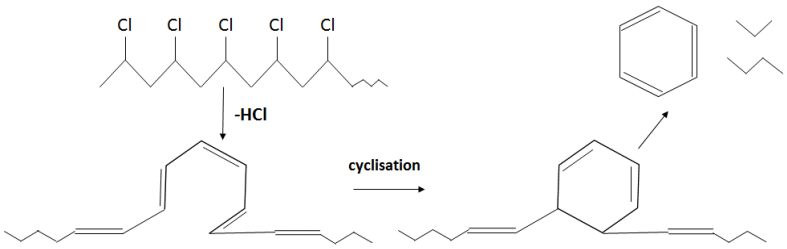

Figure 4. Schematic cyclisation reaction during PVC pyrolysis (adapted from [28]).

Preprints (www.preprints.org) | NOT PEER-REVIEWED | Posted: 24 October 2018 doi:10.20944/preprints201810.0581.v1

Peer-reviewed version available at Recycling 2018, 3, 57; doi:10.3390/recycling3040057

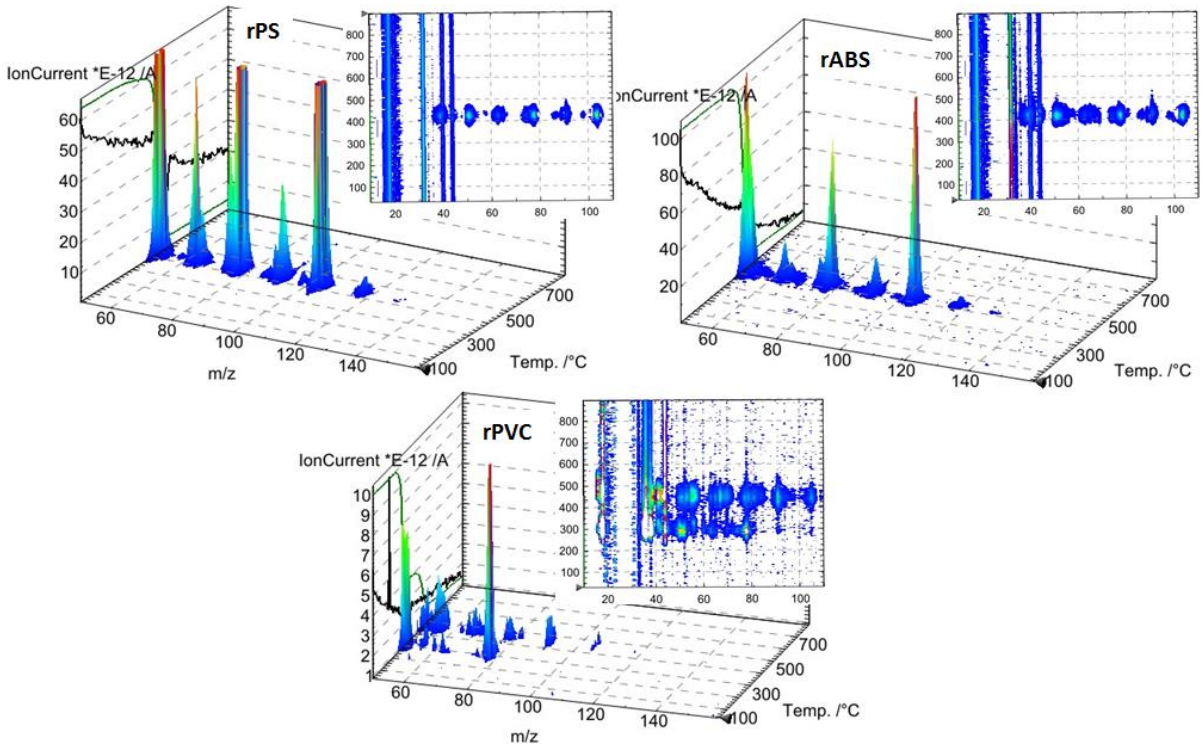

Figure 5. TGA MS analysis of rPS, rABS and rPVC.

References

1. Plastics-the Facts 2017. An analysis of European plastics production, demand and waste data. PlasticsEurope.

2. eur-lex.europa.eu/legal-content/EN/TXT/?qid=1516265440535&uri=COM:2018:28:FIN.

3. Huysman, S.; Sala, S.; Mancini, L.; Ardente, F.; Alvarenga, R.A.F.; Meester, S.; Mathieux, F.; Dewulf, J. Toward a systematized framework for resource efficiency indicators. *Resources, Conservation and Recycling* **2015**, 95, 68–76, doi:10.1016/j.resconrec.2014.10.014

4. REACH Restrictions, European Commission, 2009.

5. Quaghebeur. M.; Laenen, B.; Geysen, D.; Nielsen, P.; Pontikes, Y.; Van Gerven, T.; Spooren, J. Characterization of landfilled materials: screening of the enhanced landfill mining potential. *Journal of Cleaner Production* **2013**, 55, 72–83, doi:10.1016/j.jclepro.2012.06.012.

6. Rayna, T.; Striukova, L. From rapid prototyping to home fabrication: How 3D printing is changing business model innovation. *Technological Forecasting & Social Change* **2016**, 102, 214–224, doi:10.1016/j.techfore.2015.07.023.

7. Baechler, C.; DeVuono, M.; Pearce, J.M. Distributed recycling of waste polymer into RepRap feedstock. *Rapid Prototyping Journal* **2013**, 19(2), 118–125, doi:10.1108/13552541311302978

8. www.3d-printer-filaments.com

9. www.bigrep.com

10. Mirón. V.; Ferrándiz, S.; Juárez, D.; Mengual, A. Manufacturing and characterization of 3D printer filament using tailoring materials. *Procedia Manufacturing* **2017**, 13, 888–894, doi:10.1016/j.promfg.2017.09.151.

11. Zander, N.E.; Gillan, M.; Lambeth, R.H. Recycled polyethylene terephthalate as a new FFF feedstock material. *Additive Manufacturing* **2018**, 21, 174–182, doi:10.1016/j.addma.2018.03.007

12. https://webbook.nist.gov/chemistry/

13. www.channelpa.com https://www.channelpa.com/download-product-pdf/index.php?id=54649&name=MAGNUM%E2%84%A2%208391

14. http://www.irpcmarket.com/upload/document/datasheet-1311650225.pdf ASTM

15. www.merck.com

16. https://plastics.ulprospector.com/generics/46/c/t/polyvinyl-chloride-pvc-properties-processing/sp/8

17. Jin, H.; Gonzales-Gutierrez, J.; Oblak, P.; Zupancic, B.; Emri, I. Effect of extensive recycling on flow properties of LDPE. ANTEC ® **2013**, 98–101.

18. Wang, J.; Li, Y.; Song, J.; He, M.; Song, J.; Xia, K. Recycling of acrylonitrile-butadiene-styrene (ABS) copolymers from waste electrical and electronic equipment (WEEE), through using an epoxy-based chain extender. *Polymer Degradation and Stability* **2015**, 112, 167–174, doi:10.1016/j.polymdegradstab.2014.12.025.

19. Olmos, D.; Martén, E.V.; González-Benito, J. New molecular-scale information on polystyrene dynamics in PS and PS-$BaTiO_3$ composites from FTIR spectroscopy. *Physical Chemistry Chemical Physics* **2014**, 16, 24339–24349, doi:10.1039/c4cp03516j.

20. Tiganis, B.E.; Burn, L.S.; Davis, P.; Hill, A.J. Thermal degradation of acrylonitrile-butadiene-styrene (ABS) blends. *Polymer Degradation and Stability* **2002**, 76, 425–434, doi:10.1016/S0141-3910(02)00045-9.

21. Mallakpour, S.; Sadaty, M.A. Thiamine hydrochloride (vitamin B_1) as modifier agent for TiO_2 nanoparticles and the optical, mechanical and thermal properties of poly(vinyl chloride) composite film. *RSC Advances* **2016**, 6, 92596–92604, doi:10.1039/c6ra18597e.

22. www.asminternational.org/documents/10192/1883419/amp

23. www.shimadzu.com/an/industry/petrochemicalchemical/chem0201010.htm

24. www.misumi-techcentral.com/tt/en/mold/2011/12/106-glass-transition-temperature-tg-of-plastics.html.

25. Castro, A.; Soares, D.; Vilarinho, C.; Castro, F. Kinetics of thermal de-chlorination of PVC under pyrolytic conditions. *Waste Management* **2012**, 32, 847–851.

26. Starnes, W.H. Structural and mechanical aspects of the thermal degradation of poly(vinyl chloride). *Progress in Polymer Science* **2002**, 27, 2133–2170, doi:10.1016/j.wasman.2015.11.041.

27. Carty, P.; White, S. Char formation in polymer blends. *Polymer* **1994**, 35(2), 343–347, doi:10.1016/0032-3861(94)90701-3.

28. Slapak, M.J.P.; Kasteren, J.M.N.; Drinkengburg, A.A.H. Determination of the pyrolytic degradation kinetics of virgin-PVC and PVC-waste by analytical and computational methods. *Computational and Theoretical Polymer Science* **2000**, 10, 481–489, doi:10.1016/S1089-3156(99)00055-0.

29. Miranda. R.; Yang, J.; Roy, C.; Vasile, C. Vacuum pyrolysis of PVC I. Kinetic study. *Polymer Degradation and Stability* **1999**, 64, 127–144, doi:10.1016/S0141-3910(98)00186-4.

30. Matsuzawa Y, Ayabe M, Nishino J, Kubota N, Motegi M. Evaluation of char fuel ratio in municipal pyrolysis waste. *Fuel* **2004**, 83, 1675–1687, doi:10.1016/j.fuel.2004.02.006.

31. Schartel, B.; Kunze, R.; Neubert, D.; Tidjani, A. ZnS fire retardant in plasticized PVC. *Polymer International* **2002**, 51, 213–222, doi:org/10.1002/pi.845.

32. Xu, J.; Liu, C.; Qu, H.; Ma, H.; Jiao, Y.; Xie J. Investigation on the thermal degradation of flexible poly(vinyl chloride) filled with ferrites as flame retardant and smoke suppressant using TGA-FTIR and TGA-MS. *Polymer Degradation and Stability* **2013**, 98, 1506–1514, doi:10.1016/j.polymdegradstab.2013.04.016.

33. McNeill, I.C.; Memetea, L.; Cole, W.J. A study of the products of PVC thermal degradation. *Polymer Degradation and Stability* **1995**, 49, 181–191.

34. Suzuki, M.; Wilkie, C.A. The thermal degradation of acrylonitrile-butadiene-styrene terpolymer as studied by TGA/FTIR. *Polym Degrad Stab* **1995**, 47, 217–221.

35. www.perkinelmer.com/labsolutions/resources/docs/APP_009908_01_Characterization_of_Polymers_using_TGA.pdf

36. http://www.thermal-instruments.co.uk/ABR_PVCbyTG-GCMS.pdf

37. Chigwada, G.; Kandare, E.; Wang, D.; Majoni, S.; Mlambo, D.; Wilkie, C.A.; Hossenlopp, J.M. Thermal stability and degradation kinetics of polystyrene/organically-modified montmorillonite nanocomposites. *J Nanoscience Nanotechnology* **2008**, 8(4), 1927–1936.

38. Özsin, G.; Pütün, A.E. Insights into pyrolysis and co-pyrolysis of biomass and polystyrene: Thermochemical behaviors, kinetics and evolved gas analysis. *Energy Conversion and Management* **2017**, 149, 675–685.

39. Seleem, S.; Hopkins, M.; Olivio, J.; Schiraldi, D.A. Comparison of thermal decomposition of polystyrene products vs. bio-based polymer aerogels. OHIO J SCI **2017**, 117(2), 50–60.

40. Saraji-Bozorgzad, M.; Geissler, R.; Streibel, T.; Mühlberger, F.; Sklorz, M.; Kaisersberger, E.; Denner, T.; Zimmermann, R. Thermogravimetry coupled to single photon

ionization quadrupole mass spectrometry: A tool to investigate the chemical signature of thermal decomposition of polymeric materials. *Anal Chem* **2008**, 80, 3393–3403.

41. www.hitachi- hightech.com/file/global/pdf/products/science/appli/ana/thermal/application_TA_066e.pdf

42. Vouvoudi, E.C.; Rousi, A.T.; Achilias, D.S. Thermal degradation characteristics and products obtained after pyrolysis of specific polymers found in Waste Electrical and Electronic Equipment. *Front Environ Sci Eng* **2017**, 11(5), 1–10.

43. Matuana, L.M.; Kamdem, D.P.; Zhang, J. Photoaging and stabilization of rigid PVC/wood-fiber composites. *J Appl Polym Sci* **2001**, 180, 943–960.

44. www.smithersrapra.com/SmithersRapra/media/Sample-Chapters/Physical-Testing-of-Plastics.pdf